

Evolution of the Southern Quesnel Arc: Potential to Distinguish Variability in Magmatic Porphyry Fertility, South-Central British Columbia (NTS 082E, L, 092H, I, P, 093A, B)

T.J. Ledoux¹, MDRU – Mineral Deposit Research Unit, The University of British Columbia, Vancouver, British Columbia, tledoux@eoas.ubc.ca

C.J.R. Hart, MDRU – Mineral Deposit Research Unit, The University of British Columbia, Vancouver, British Columbia

Ledoux, T.J. and Hart, C.J.R. (2021): Evolution of the southern Quesnel arc: potential to distinguish variability in magmatic porphyry fertility, south-central British Columbia (NTS 082E, L, 092H, I, P, 093A, B); *in* Geoscience BC Summary of Activities 2020: Minerals, Geoscience BC, Report 2021-01, p. 75–90.

Introduction

Porphyry Cu deposits are the world's largest repositories of Cu and Mo, and are major sources of Au and Ag (International Copper Study Group, 2019). Most porphyry Cu deposits have a spatial and temporal association with active plate margins, such as the continental-margin arc along western North and South America. Porphyry Cu deposits are critical contributors to the British Columbia (BC) economy. In 2018, 293.5 kt of Cu concentrate was extracted from BC porphyry deposits, equating to over \$2 billion in annual revenues and contributing more than half of Canada's Cu production (Natural Resources Canada, 2018; PricewaterhouseCoopers Inc., 2019).

The most fundamental process in forming large porphyry Cu deposits is the exsolution of hydrothermal fluids from magma in large, crystallizing, midcrustal batholiths below the site of porphyry Cu deposit formation (Dilles and Einaudi, 1992). These fluids accumulate Cl, S and metals that preferentially partition from the magma to the fluid, and together they buoyantly stream through the upper crust to where gases exsolve and break the rock. With decreasing temperature, fluids condense and precipitate silicate and sulphide minerals to form porphyry Cu deposits.

Formation of an economic porphyry Cu deposit is dependent on six key magmatic parameters: 1) oxidation state, 2) temperature, 3) water content, 4) metal content, 5) chlorine content, and 6) sulphur content (Burnham and Ohmoto, 1980). A magma may be considered fertile and therefore capable of generating an economic deposit if it 1) is oxidized, 2) cooled quickly, 3) has a high water content, 4) contains enough Cu±Au±Mo, 5) has enough Cl to transport Cu in solution, and 6) has enough S (and Fe) to

precipitate Cu-sulphide minerals. Research in mineral chemistry by Ballard et al. (2002), Lee (2008), Celis (2015), Dilles et al. (2015), Bouzari et al. (2016), Williamson et al. (2016) and Lee et al. (2020) has identified trace-element signatures and grain morphology of zircon, apatite, titanite and plagioclase that correlate with many attributes of magma fertility. For example, indicators of a magma's oxidation state and water content are recorded in and reflected by the characteristics and compositions of magmatic zircon grains. As a result, zircon grains, in addition to being robust U-Pb geochronometers, can also provide insights that contribute to evaluating the fertility of its host magmas and ultimately to exploration decision-making.

Previous research in magmatic porphyry fertility focused primarily on zircon composition and variability within a single deposit, pluton or mineral district (e.g., Wainright et al., 2011; Lee et al., 2017; Kobylinski et al., 2020; Lee et al., 2020), or more generally compared the signatures of fertile and barren plutonic rocks from different and tectonically unrelated locations (Belousova et al., 2006; Dilles et al., 2015; Lu et al., 2016). Some recent research (e.g., Shen, 2015; Rezeau et al., 2019; Bouzari et al., 2020; Pizzaro et al., 2020) has examined magmatic porphyry fertility of numerous bodies within a belt or arc. These studies demonstrate the variability of zircon as a porphyry-fertility indicator within an arc, although further research is needed to establish the scale of variability within an evolving arc, along an arc segment or across a migrating arc. How do zircon magmatic-fertility indicators vary between arcs or arc segments with different basements, or with different crustal thicknesses, or within an arc in time and space?

The authors anticipate that there would be links between the fertility characteristics and the petrogenetic, magmatic and tectonic processes that control the magma formation. Porphyry deposits can be formed from calcalkaline, high-K, silica-saturated alkaline, silica-undersaturated alkaline and even tholeiitic diorites, and high-silica granites (Mo

¹The lead author is a 2020 Geoscience BC Scholarship recipient.

This publication is also available, free of charge, as colour digital files in Adobe Acrobat® PDF format from the Geoscience BC website: <http://geosciencebc.com/updates/summary-of-activities/>.

deposits), so their associated mineral chemistry signatures are expected to vary. The ability to identify fertile-arc magmas and understand variability within and between different arc settings will enable explorers to better recognize those magmas that have the potential to form an economic porphyry Cu deposit, and to differentiate them from barren magmas.

Since the BC phase of the project just started with field sampling, this paper provides appropriate background geological information and context for the samples, as well as sample descriptions, as a foundation for subsequent analytical results.

Geological Setting

Much of British Columbia is underlain by a series of Mesozoic island-arc and associated accretionary-margin assemblages that were accreted onto the ancestral North American margin. Porphyry Cu deposits in the Canadian Cordillera formed mainly during two separate time periods in response to different tectonic settings: Early Mesozoic (Late Triassic to Middle Jurassic) deposits are associated with calcalkaline to alkaline intrusive suites that formed in the Stikinia and Quesnellia island-arc settings prior to their accretion onto continental North America; and younger Mesozoic–Cenozoic (Late Cretaceous to Eocene) calcalkaline deposits were emplaced into previously accreted terranes that formed the western North American continental margin (McMillan et al., 1996).

Quesnellia comprises Middle Triassic to Early Jurassic island-arc assemblages and related intrusions that, in part, unconformably overlie late Paleozoic island-arc and oceanic subterrane (Figure 1; Read and Okulitch, 1977; Smith, 1979). Quesnellia was accreted onto ancestral North America in the Early Jurassic (~186 Ma; Nixon et al., 1993). The late Paleozoic through mid-Mesozoic oceanic Cache Creek terrane is faulted against the western margin of Quesnellia as an accretionary mélangé above an east-dipping subduction zone (Travers, 1978). Eastern Quesnellia is marked by unconformable contacts on the Slide Mountain terrane oceanic sedimentary rocks and the adjacent pericratonic Harper Ranch subterrane and Kootenay terrane (Colpron and Price, 1995).

Southern Quesnellia Arc

The lower parts of Mesozoic Quesnellia are composed primarily of the Middle to Late Triassic Nicola Group volcanic arc in the west and the coeval Slocan Group siliciclastic basin to the east (Little, 1960; Preto, 1979). Preto (1979) recognized that the Nicola Group formed parallel, linear, fault-bounded magmatic belts between Merritt and Princeton. McMillan (1981) and Monger (1985) expanded this classification farther north to Kamloops and recognized a new eastern sedimentary belt and a few good stratigraphic

contacts. Mortimer (1987) determined that the older volcanic rocks in the western belt of the southern Nicola Group are type-2, low- to medium-K, calcalkaline to tholeiitic rocks; and younger volcanic rocks in the central and eastern belts of the Nicola Group are type-1, high-K, shoshonitic, calcalkaline to alkaline rocks. Schiarizza (2016) established a stratigraphic framework of the Nicola Group in the Bridge Lake–Quesnel River area, breaking it into four assemblages that define a regional syncline and roughly correlate with the belts first described by Preto (1979) farther to the south.

Assemblage 1 of Schiarizza (2016) correlates with the eastern sedimentary belt, is Middle to Late Triassic based on conodonts (Struik, 1988; Schiarizza et al., 2013), and is exposed along the eastern margin of the Nicola belt. This assemblage consists of basinal sedimentary rocks with lesser volcanoclastic and basaltic rocks. Assemblage 2 correlates with the western volcanic belt, is Late Triassic based on conodonts and macrofossils (Schiarizza, 2016), and defines the west and east limbs of a regional syncline in the north and spans the west limb of the Nicola Group in the south. This assemblage is composed of volcanoclastic rocks, locally intercalated with subaerial pyroxene-phyric basalt, epiclastic sedimentary rocks and limestone. Assemblage 3 correlates with the central volcanic belt, is inferred to be Norian based on the stratigraphic position between Assemblages 2 and 3, and crops out as two belts in the north and spans the centre of the Nicola Group in the south. This assemblage consists primarily of pyroxene-phyric basalt and andesite, with lesser interbedded sedimentary rocks in the southern portion of the Nicola Group. Assemblage 4 correlates with the eastern volcanic belt, is Late Triassic based on a U-Pb zircon date of 203.9 ± 0.4 Ma from a plagioclase-phyric andesite (Schiarizza et al., 2013), unconformably overlies the rest of the Nicola Group as the central belt in the north, and is fault bounded between the central volcanic belt and eastern sedimentary belt in the south. This assemblage consists of polymictic conglomerate with abundant plutonic rocks, sandstone, basalt and andesite (Preto, 1979; Schiarizza, 2019).

Southern Quesnellia Plutonism

The magmatic axis of Late Triassic to Early Jurassic Quesnellia plutonism migrated episodically eastward, constructing three subparallel linear plutonic axes (Table 1; Schiarizza, 2014). The plutonic episodes occurred over an ~36 m.y. period (229–193 Ma; Parrish and Monger, 1992; Kobylinski et al., 2020) as part of the longer, ~54 m.y. period (247–193 Ma; Schiarizza, 2019) of arc evolution above an east-dipping subduction zone. As the magmatic axis moved toward the back arc in the east, plutonic episodes evolved from a calcalkaline affinity to an alkaline affinity, and back to calcalkaline; and porphyry-deposit metal assemblages transitioned from Cu-Mo to Cu-Au and back

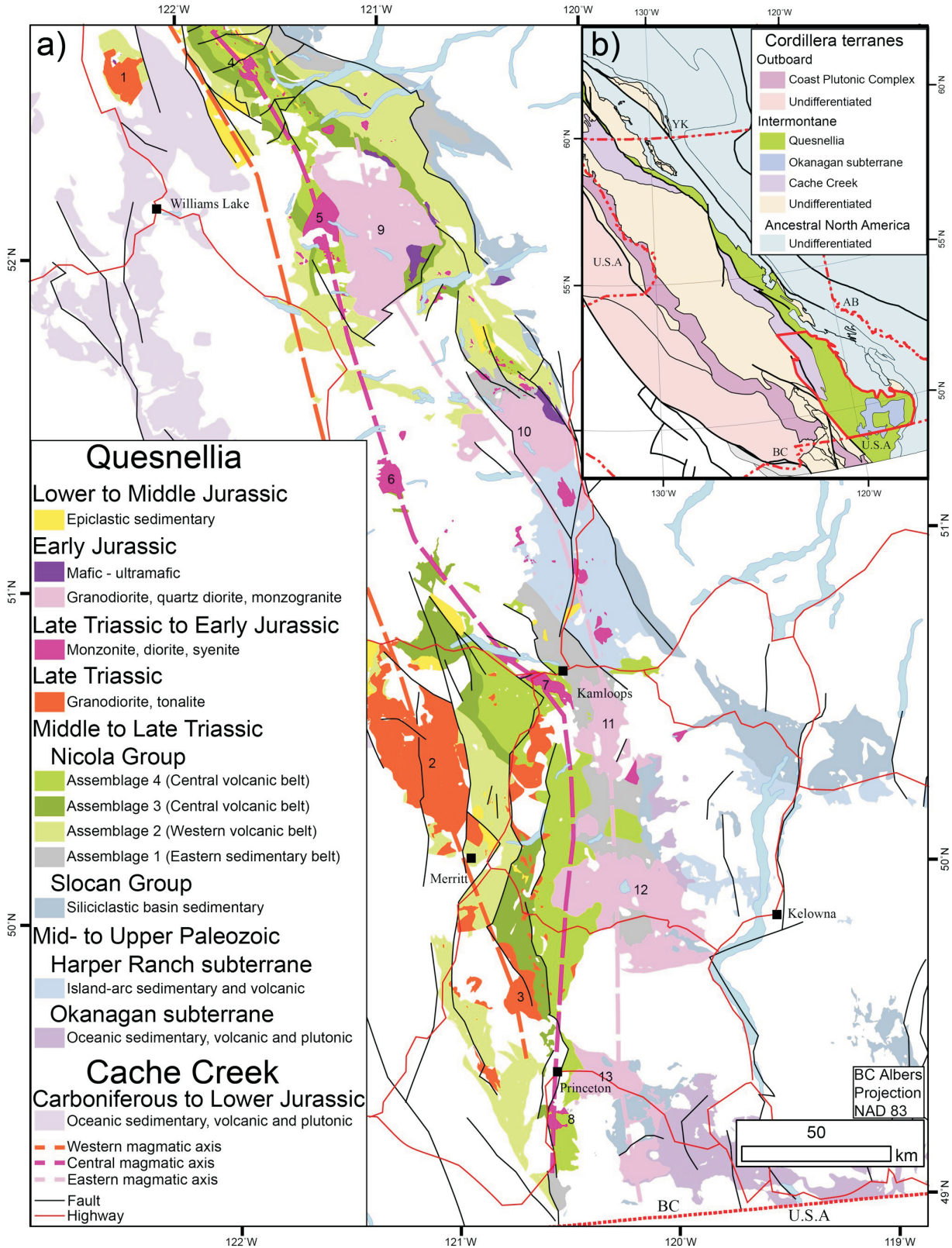


Figure 1. a) Geology of southern Quesnellia and the Cache Creek terrane, south-central British Columbia (modified after Cui et al., 2017). Nicola Group assemblages after Preto (1979), McMillan (1981), Monger (1985) and Schiarizza (2019). Symbols: red dashed line, Western magmatic axis; fuchsia dashed line, Central magmatic axis; pink dashed line, Eastern magmatic axis (modified after Schiarizza (2014)). Numbers: 1, Granite Mountain batholith; 2, Guichon Creek batholith; 3, Alice Lake pluton; 4, Mount Polley; 5, Spout Lake pluton; 6, Rayfield River; 7, Iron Mask batholith; 8, Copper Mountain; 9, Takomkane batholith; 10, Thuya batholith; 11, Wild Horse batholith; 12, Pennask batholith; 13, Bromley batholith. **b)** Terranes of British Columbia (modified after Colpron and Nelson, 2020).

to Cu-Mo (Logan and Mihalynuk, 2014; Schiarizza, 2014). Most Quesnellia porphyry deposits formed between 210 and 195 Ma, with an especially prolific 6 m.y. long mineralizing event centred at 205 Ma (Mortensen et al., 1995).

Western Magmatic Axis (Late Triassic Calcalkaline Plutonism)

The Western magmatic axis is characterized by plutonism of Late Triassic age (229–206 Ma; D’Angelo et al., 2017; Kobylinski et al., 2020; Lee et al. 2020), specifically calcalkaline granodiorite-tonalite suite intrusive rocks and associated Cu-Mo porphyry deposits. Intrusions here are large (up to 2000 km²), thick (>6 km), consist of multiple concentrically zoned phases and were typically emplaced at depths of ~5 km (Sutherland Brown, 1976). The Guichon Creek and Granite Mountain batholiths are the main intrusions that define this magmatic axis; they were emplaced into Assemblage 2 of the Nicola group. These bodies also host the giant Highland Valley Copper and Gibraltar porphyry Cu districts, respectively. Several other intrusive bodies, such as the Nicola batholith, Alice Lake pluton and other smaller intrusions southeast of the Guichon Creek batholith, make up a contemporaneous but smaller volume subset within the rest of the Western magmatic axis. Much of the Western magmatic axis between the Guichon Creek batholith and the Granite Mountain batholith is covered in Cenozoic volcanic and sedimentary units that could overlie potentially prolific porphyry Cu-hosting intrusions.

Guichon Creek Batholith

The Late Triassic Guichon Creek batholith, 65 km southwest of Kamloops, trends north, measures 65 by 30 km and was emplaced at depths between 2.6 and 7.4 km in Assemblage 2 of the Nicola group (Northcote, 1969; McMillan, 1976, 1985; Byrne et al., 2013; D’Angelo, 2016) as a flattened funnel shape with an average thickness of 6 km on the

edges and a maximum thickness of >12 km at the centre (Ager, 1974). The batholith is calcalkaline, composite and concentrically zoned (McMillan, 1976), comprising an earlier granodioritic to quartz monzonitic stock on the edge (218 ±0.18 Ma; Lee et al., 2020) and a larger zoned batholith in the centre that youngs from a quartz diorite phase at the margin (211.2 ±0.17 Ma) to a predominantly granodiorite core (206.95 ±0.22 Ma; D’Angelo et al., 2017). The margin of the batholith is composed of heterogeneous, equigranular gabbroic to monzodioritic rocks that include minor olivine, orthopyroxene and clinopyroxene in the gabbroic phases and abundant hornblende and minor quartz in the dioritic phases. Toward the core of the batholith, the rocks transition from equigranular granodiorite through porphyritic granodiorite to monzogranite with a few percent of mafic minerals. Mafic minerals in the units at the margin of the batholith are pyroxenes with hornblende rims and hornblende with relict cores of pyroxene. Mafic minerals in the units near the core of the batholith comprise hornblende and biotite, and, at the core of the batholith, only biotite phenocrysts (Byrne et al., 2013; D’Angelo et al., 2017).

The Guichon Creek batholith hosts five deposits related to two mineralization events: an ~210 Ma event that formed the deposits in the Bethlehem area (Ash et al., 2007; Byrne et al., 2013) and a 208.4 ±0.9 Ma event that formed the Valley, Lornex, Highmont and J.A. deposits (D’Angelo et al., 2017). The Highland Valley deposits contained 6.2 Mt Cu, between the 4.89 Mt of Cu production over the last 35 years (BC Geological Survey, 2020) and a current resource of 484 Mt at 0.28% Cu and 0.009% Mo (Teck Resources Limited, 2019).

Table 1. Characteristics of the Western, Central, and Eastern magmatic axes of the Quesnellia arc. * indicates inferred resources. All other resources are measured and indicated.

	Western magmatic axis	Central magmatic axis	Eastern magmatic axis
Age (Ma)	229–206	204–200	202–193
Magmatic affinity	Calcalkaline	Alkaline	Calcalkaline, high-K calcalkaline
Predominant rock type	Granodiorite and tonalite	Diorite and monzonite	Granodiorite and quartz diorite
Average batholith dimensions: length x width x thickness (km)	42 x 23 x 8	16 x 7 x 4	32 x 33
Average emplacement depth (km)	5	1	4
Major porphyry districts	Highland Valley and Gibraltar	Copper Mountain, Afton-Ajax, and Mount Polley	Brenda and Woodjam
Metal assemblages	Cu-Au-Mo	Cu-Au	Cu-Mo ± Au
Historical copper production (Mt)	6.39	1.83	0.28
Current copper resource (Mt)	2.81	4.1	0.79*
Total contained copper (Mt)	9.2	5.93	1.07

* inferred resource

Granite Mountain Batholith

The Late Triassic Granite Mountain batholith, 60 km north of Williams Lake, measures 18 by 10 km and was emplaced at a depth of ~5 km (Sutherland Brown, 1976). The batholith was originally considered to intrude the Cache Creek terrane (Bysouth et al., 1995), but mapping by Schiarizza (2014) identified Assemblage 2 Nicola Group rocks on the margins of the batholith, indicating that it is part of Quesnellia. The batholith is calcalkaline and composite (Panteleyev, 1978), and comprises multiple tonalitic to dioritic intrusions that have gradational contacts. In the north, it is composed of tonalite with quartz > plagioclase and 5–10% mafic minerals (biotite > hornblende) that grades to a more mafic tonalite near the centre and to a border phase at the southern margin that is composed of equigranular quartz diorite grading locally into tonalite or diorite with >25% hornblende. The northeastern margin consists of an older composite stock of equigranular tonalite and variably equigranular to porphyritic tonalite and diorite (Schiarizza, 2015). The batholith was constructed over an ~25 m.y. period beginning at 229.2 ±4.4 Ma with crystallization of barren tonalite and followed by emplacement of multiple mineralizing tonalitic intrusions from 218.9 ±3.1 to 205.8 ±2.1 Ma (Kobylnski et al., 2020).

The Granite Mountain batholith hosts the Gibraltar Cu-Mo porphyry deposit that consists of a cluster of three chimney-like orebodies (Ash and Riveros, 2001), formed during multiple, distinct, magmatic-hydrothermal events that have Re-Os ages on molybdenite ranging from 215.0 ±1.0 to 210.1 ±0.9 Ma (Harding, 2012). The Gibraltar deposit contained 3.0 Mt of Cu, between the 1.5 Mt of Cu extracted from the Gibraltar mine (BC Geological Survey, 2020) and the current resource of 594 Mt at 0.25% Cu and 0.008% Mo (Weymark, 2019).

Central Magmatic Axis (Late Triassic to Early Jurassic Alkaline Plutonism)

The Central magmatic axis is characterized by plutonism of latest Triassic to Early Jurassic (204–200 Ma; Mortensen et al., 1995), alkaline, silica-saturated to -undersaturated intrusive rocks of the syenite-diorite suite containing Au-rich Cu-Au deposits. The Mount Polley, Spout Lake and Rayfield River intrusive complexes, Iron Mask batholith and Copper Mountain intrusive complex are the main intrusions that define the Central magmatic axis. The Copper Mountain intrusion and the Iron Mask batholith are silica saturated and locally silica undersaturated, whereas the Mount Polley and Rayfield River intrusions are silica undersaturated (Lang et al., 1995). The Iron Mask batholith hosts a number of Cu-Au occurrences, most notably the Afton and Ajax deposits; and the Copper Mountain and Mount Polley intrusive complexes each host a porphyry Cu-Au district of the same name.

Copper Mountain Intrusive Complex

The Early Jurassic Copper Mountain intrusive complex is located 15 km south of Princeton, measures 8 by 6 km and was emplaced in a subvolcanic environment in Assemblage 4 of the Nicola Group (Preto, 1972; Schiarizza, 2019) at a depth of ~1.1 km (Sutherland Brown, 1976). This intrusive complex is composed of multiple alkalic stocks and dike swarms. The Copper Mountain stock, in the southern part of the intrusive complex, is concentrically differentiated and grades from equigranular clinopyroxene diorite with local gabbro at the margins through clinopyroxene-biotite monzonite to inequigranular syenite at the core (Holbek and Joyes, 2013). Zircons from the monzodiorite in the Copper Mountain stock have a U-Pb age of 202.7 ±4.4 Ma (Mortensen et al., 1995). The Smelter Lake and Voight stocks are in the northeastern and northwestern parts of the intrusive complex, respectively, and are composed of nearly identical equigranular biotite-clinopyroxene diorite. The Lost Horse intrusive complex, situated between these stocks, is a nearly continuous mass of dikes composed of 1) porphyritic syenite to diorite that consist of euhedral plagioclase, subhedral to anhedral clinopyroxene and varying amounts of interstitial alkali feldspar and biotite; and 2) trachytic latite and trachyte to porphyritic micromonzonite and microsyenite that consist of euhedral plagioclase and clinopyroxene, well-formed biotite and interstitial alkali feldspar (Preto, 1972).

Since production at the Copper Mountain mine began in 1917, 1.05 Mt of Cu and 28.5 t of Au have been mined from the Copper Mountain and Ingerbelle deposits (BC Geological Survey, 2020). These deposits have a combined remaining resource of 584 Mt of 0.23% Cu and 0.1 g/t Au (Copper Mountain Mining Corp., 2020), making for a total of 2.34 Mt Cu and 82.9 t Au in past production and current resources.

Iron Mask Batholith

The Late Triassic to Early Jurassic Iron Mask batholith southwest of Kamloops is a 35 by 5 km, northwest-trending intrusion (Logan and Mihalynuk, 2005) that was emplaced at a depth of ~0.9 km (Sutherland Brown, 1976) as a 2–6 km thick, elongate, funnel-shaped body (Ager, 1974; Thomas, 2019). The batholith was apparently emplaced in a comagmatic environment of alkaline volcanic rocks of Nicola Group Assemblage 4 (Northcote, 1978; Schiarizza, 2019). The Iron Mask batholith is a polyphase alkalic intrusive complex composed of the Pothook, Cherry Creek, Sugarloaf and Hybrid phases. The Pothook phase is an equigranular biotite-pyroxene diorite with 25% clinopyroxene, 22% biotite and magnetite; the Cherry Creek phase is an equigranular biotite monzonite; the Sugarloaf phase is a porphyritic plagioclase- and hornblende-phyric diorite; and the Hybrid phase is a xenolith-rich phase that marks the contacts between the three intrusions and the sur-

rounding Nicola Group country rock, and is composed primarily of Nicola Group xenoliths in a matrix of the Pothook phase and locally the Cherry Creek and Sugarloaf phases (Snyder and Russell, 1995; Logan and Mihalynuk, 2005). The Pothook and Cherry Creek phases are Late Triassic with zircon U-Pb ages of 204.7 ± 3 and 204.5 ± 0.6 Ma, respectively, and the Sugarloaf diorite has a slightly younger Ar/Ar cooling date of 200.1 ± 2.5 Ma (Logan et al., 2007).

The Iron Mask batholith hosts the currently producing New Afton Cu-Au-Ag mine, which is directly beneath the historical Afton open pit (New Gold Inc., 2019), and multiple past-producing Cu-Au deposits that include the Ajax West, Ajax East, Crescent, Pothook and Python-Makao deposits (Lang and Stanley, 1995). Porphyry Cu-Au deposits are associated with all three phases of the Iron Mask batholith. A total of 0.51 Mt Cu and 38.9 t Au have come from historical production from the Afton, Ajax, Crescent and Pothook deposits, with a majority coming from Afton (Logan and Mihalynuk, 2005; BC Geological Survey, 2020). Ajax has a remaining resource of 442.3 Mt of 0.29% Cu and 0.19 g/t Au (Ghaffari et al., 2009) and Afton has a remaining reserve of 47.3 Mt of 0.77% Cu and 0.66 g/t Au, and a resource of 57 Mt of 0.74% Cu and 0.61 g/t Au (New Gold Inc., 2019), making for a combined remaining resource of 2.06 Mt Cu and 113.3 t Au. All of the deposits in the Iron Mask batholith contained a total of 2.57 Mt Cu and 152.2 t Au in past production and current resources.

Eastern Magmatic Axis (Early Jurassic Calcalkaline Plutonism)

The Eastern magmatic axis is characterized by Early Jurassic (202–193 Ma; Parrish and Monger, 1992; Schiarizza et al., 2009), calcalkaline to high-K calcalkaline intrusive rocks of the granodiorite–quartz diorite suite, containing Cu-Mo deposits. The eastern axis is defined by the large, composite and zoned Bromley, Pennask, Wild Horse, Thuya and Takomkane batholiths. The Pennask and Takomkane batholiths host the past-producing Brenda Cu-Mo mine and Woodjam district, respectfully. This axis also includes several smaller granite to diorite plutons farther east, such as the Cahill Creek pluton and Hedley intrusion, in addition to several smaller, concentrically zoned, Alaskan-type ultramafic bodies that intrude the Nicola Group along the easternmost margins of the axis.

Pennask Batholith

The Early Jurassic Pennask batholith, 35 km west of Kelowna, measures 38 by 50 km and was emplaced into Nicola Group Assemblages 1 and 4 (Soregaroli and Whitford, 1976; Schiarizza, 2019) at a depth of ~4.6 km (Sutherland Brown, 1976). The batholith is composed of poly-phase granodiorite and quartz diorite with a U-Pb zircon date of 194 ± 1 Ma (Parrish and Monger, 1992). Within the ‘Brenda stock’, an informal subdivision within the much larger batholith, quartz diorite is equigranular with

euhedral acicular hornblende > anhedral biotite; and granodiorite is equigranular to inequigranular with anhedral biotite = euhedral acicular hornblende. The contact between the two units is typically diffuse, but, where sharp, the granodiorite is chilled against the quartz diorite (Soregaroli and Whitford, 1976; this study).

The Brenda Cu-Mo deposit is located near the margin of the batholith and is hosted within the Brenda stock. The deposit formed over a period of less than 1 m.y., based on a 193.9 ± 0.9 Ma Re-Os model age of molybdenite taken from one of the younger vein sets (Logan et al., 2011). The Brenda mine produced 0.28 Mt of Cu and 0.07 Mt of Mo from 177 Mt of ore grading 0.17% Cu and 0.043% Mo throughout the 20-year mine life (Weeks et al., 1995; BC Geological Survey, 2020).

Takomkane Batholith

The latest Triassic to Early Jurassic Takomkane batholith, located 50 km east of Williams Lake, measures 50 by 40 km and was emplaced in Assemblages 2, 3 and 4 of the Nicola Group and the Spout Lake pluton (Schiarizza, 2019) at a depth of ~3 km (del Real et al., 2017). The batholith is a calcalkaline composite intrusion, consisting of the Boss Creek, Schoolhouse Lake and Woodjam Creek units (Schiarizza et al., 2009). The Boss Creek unit, dated at 202.5 ± 0.5 and 199.6 ± 0.3 Ma (Schiarizza et al., 2009), is an equigranular quartz monzodiorite to granodiorite that locally grades into quartz diorite and diorite. The unit is typically composed of 15–25% mafic minerals, typically consisting of hornblende > biotite, and local clinopyroxene. The Schoolhouse Lake unit, dated at 193.5 ± 0.6 Ma (Whiteaker et al., 1998) and 195.0 ± 0.4 Ma (Schiarizza et al., 2009), is an inequigranular granodiorite to monzogranite that is characterized by alkali-feldspar megacrysts with 10–20% mafic minerals, consisting of hornblende > biotite. The Woodjam Creek unit (197.48 ± 0.44 to 194.99 ± 0.16 Ma; del Real et al., 2017) is equigranular to locally inequigranular granodiorite, monzogranite, quartz monzonite and quartz monzodiorite with 10–15% mafic minerals, consisting of hornblende > biotite (Schiarizza et al., 2009).

The Woodjam Creek unit hosts the Woodjam district, which is a cluster of Early Jurassic Cu-Au±Mo porphyry deposits, including the Southeast Zone Cu-Mo porphyry, the Deerhorn and Megabuck Au-Cu porphyries, and the Takom and Three Firs Cu-Au porphyries. The Deerhorn and Megabuck porphyries are related to 196.48 ± 0.21 Ma, high-K calcalkaline monzonite pencil stocks that intruded the upper strata of the Nicola Group at an emplacement depth of ~1.5–2 km (del Real et al., 2017). The Southeast Zone deposit is hosted within the Woodjam Creek phase and likely formed at a depth of ~3 km (del Real et al., 2017) at 196.9 ± 0.9 Ma, based on a Re-Os model age of molybdenite by Logan et al. (2011). The Southeast Zone, Deerhorn

and Takom deposits currently have an inferred resource of 227.5 Mt of 0.31% Cu, 32.8 Mt of 0.22% Cu and 0.49 g/t Au, and 8.3 Mt of 0.22% Cu and 0.26 g/t Au, respectively (Consolidated Woodjam Copper Corp., 2013), making for a total current resource of 0.79 Mt of contained Cu.

Samples and Methods

Roadside sampling was conducted in 2018, 2019 and 2020 to collect samples that reflect the regional plutonic variability within and between the three magmatic axes of the Late Triassic to Early Jurassic southern Quesnellia arc. These samples will be supplemented with the existing zircon trace-element data on the Guichon Creek, Granite Mountain, and Takomkane batholiths completed by Bouzari et al. (2020), Lee et al. (2020) and Lee et al. (in press). Nine rock samples have been collected: one from the Alison Lake pluton in the Western magmatic axis; four from the Iron Mask batholith in the Central magmatic axis; and one from each of the Brenda stock (Pennask batholith), Bromley batholith, Cahill Creek pluton and Hedley intrusion in the Eastern magmatic axis (Table 2). The Copper Mountain intrusive complex will be sampled at a future date to better characterize the Central magmatic axis. Magnetic susceptibility of the rocks was measured using a recently calibrated, handheld KT-9 magnetic susceptibility meter. Two to four readings were taken of the exterior of each rock sample in pin mode and two readings were taken from the cut rock slabs in no-pin mode, and the averages from both sets of readings were combined.

Glacial-till and stream-sediment samples were collected to test the effectiveness of using detrital zircons as an exploration tool; to get broader representation of the Quesnellia arc and its intrusive bodies; and to increase the potential of obtaining zircons from silica-undersaturated to weakly silica-saturated intrusions, such as the Iron Mask batholith and Copper Mountain intrusive complex, that typically have low zircon yields. Till samples were taken in arid areas with low topographic relief because the streams lack sufficient energy to move clasts and are choked with organic material. Stream-sediment samples were taken from areas with sufficient topographic relief and rainfall for running water to erode and transport rock clasts and presumably mineral grains.

Four till samples were taken from the banks of small streams or roadcuts using a trowel and dry sieved to <1 mm in the field (Table 2). At the Iron Mask batholith, three till samples were taken progressively farther down ice from each other to sample an increased proportion of the Iron Mask intrusive rocks in the till relative to the Nicola Group volcanic rocks that are up ice of the batholith. One glaciofluvial-till sample was collected from down ice of the Pennask batholith.

One stream-sediment sample was collected from a major drainage that is a catchment point downstream of the Pennask batholith and was wet sieved to <1 mm in the stream (Table 2). Additional stream-sediment samples will

Table 2. Southern Quesnellia rock, glacial-till and stream-sediment samples.

Sample ID	Latitude	Longitude	Magmatic Axis	Batholith	Unit	Magnetic Susceptibility	Sample Description
18CH-ALP	49.71231	-120.61026	Western	Alice Lake Pluton		21.15	Porphyritic diorite
20TL-BC-IMR1	50.660178	-120.467954	Central	Iron Mask Batholith	Poohook Phase	116.25	Equigranular biotite-pyroxene diorite
20TL-BC-IMR3	50.550568	-120.473389	Central	Iron Mask Batholith	Cherry Creek Phase	4.86	Equigranular biotite monzonite
20TL-BC-IMR4	50.6048	-120.3779	Central	Iron Mask Batholith	Sugarloaf Phase	39.81	Porphyritic hornblende diorite
20TL-BC-IMR5	50.563915	-120.419418	Central	Iron Mask Batholith	Hybrid Phase	1.19	Xenolith-rich diorite
20TL-BC-PR1	49.89825	-119.92915	Eastern	Pennask Batholith	Brenda Stock	18.03	Equigranular hornblende-biotite granodiorite
18CH-Toronto	49.37	-120.04	Eastern		Hedley Intrusion	0.84	Equigranular pyroxene-hornblende quartz diorite
18CH-CGP	49.33771	-120.04016	Eastern	Cahill Creek Pluton		14.63	Inequigranular hornblende-biotite granite
19CH-Bromley	49.43459	-120.29439	Eastern	Bromley Batholith		21.00	Inequigranular hornblende granodiorite
20LT-BC-IMT1	50.660178	-120.467954	Central	Iron Mask Batholith			Glacial till
20LT-BC-IMT2	50.563915	-120.419418	Central	Iron Mask Batholith			Glacial till
20LT-BC-IMT3	50.606215	-120.373081	Central	Iron Mask Batholith			Glacial till
20TL-BC-PT1	49.864029	-120.929117	Eastern	Pennask Batholith			Glaciofluvial till
20TL-BC-PF1	49.89970	-119.92893	Eastern	Pennask Batholith			Stream sediment

be collected from creeks draining the Copper Mountain intrusive complex.

Sample Descriptions

Western Magmatic Axis (Calcalkaline Granodiorite-Tonalite Suite)

Alice Lake Pluton

The fresh rock is a dark green-grey, porphyritic, crowded, plagioclase-phyric diorite (Figure 2). It is composed of creamy white tabular euhedral plagioclase (60%), translucent anhedral quartz eyes (1%), small shiny black euhedral magnetite (1%), and a fine-grained matrix of dark grey-green mafic minerals (38%). Most of the outcrops of this pluton were altered, with chlorite and epidote on fracture surfaces and locally with quartz veins displaying 2–10 mm saussurite alteration selvages along the vein margins. The rock has a magnetic susceptibility of 21.15×10^{-3} SI.

Central Magmatic Axis (Alkaline, Monzodiorite Suite)

Iron Mask Batholith

Pothook Diorite

Pothook diorite forms the northwestern core of the Iron Mask batholith and is in gradational contact with the hybrid unit to the southeast and intrusive contact with the younger Cherry Creek monzonite to the north and east and the Sugarloaf diorite to the southwest (Logan and Mihalynuk, 2005). The Pothook phase hosts the past-producing Magnet mine and the Python prospect. Sample 20TL-BC-IMR1 was collected from a fractured subcrop exposed along a small creek that cuts through the 2 m of glacial-till overburden.

The fresh rock is a pale green, equigranular, medium- to coarse-grained, biotite-pyroxene diorite (Figure 3a). It is composed of subhedral white plagioclase (45%), euhedral green clinopyroxene (25%), poikilitic biotite (22%), anhedral translucent quartz (2%) and small, shiny, black euhedral grains of magnetite (2%). Plagioclase is locally sericitized and biotite grains are weakly chloritized. The rock is locally fractured, with chlorite-magnetite veinlets in the fractures. It has a magnetic susceptibility of 116.25×10^{-3} SI.

Cherry Creek Monzonite

Cherry Creek monzonite accounts for the largest proportion of the Iron Mask batholith and forms the northernmost margin, central core and southeastern edge. The Cherry Creek phase hosts the Afton mine, which is the largest porphyry deposit in the batholith, and the past-producing Crescent mine. Sample 20TL-BC-IMR3 was collected from an outcrop that was exposed along a roadcut east of Iron Mask hill (unofficial place name; UTM Zone 10U, 680616E,

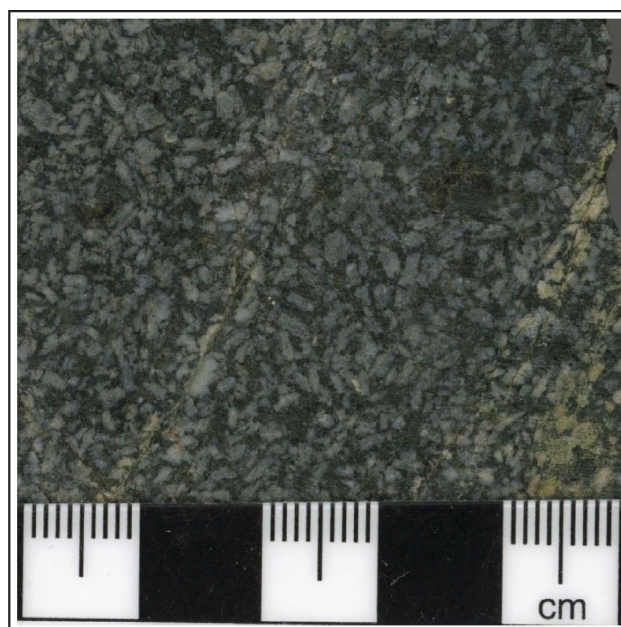


Figure 2. Porphyritic diorite of the Alice Lake pluton in the calcalkaline Western magmatic axis.

5613488N, NAD 83). The outcrop is brownish orange where not freshly exposed by the roadcut covered in black lichen.

The fresh rock is a creamy orange, equigranular, medium-grained, biotite monzonite (Figure 3b). It is composed of creamy orange subhedral alkali feldspar (56%), white subhedral plagioclase (18%), greenish black subhedral biotite (22%), translucent anhedral quartz (2%), small, shiny, black, euhedral grains of magnetite (1%), and partially to completely oxidized anhedral pyrite (1%). The rock locally contains clots (up to 1 cm) of fine-grained mafic minerals. Biotite is moderately chloritized, and the rock is weakly oxidized and has sheeted calcite veinlets. It has an average magnetic susceptibility of 4.86×10^{-3} SI that increases to 8.3×10^{-3} SI if results from oxidized rocks are excluded.

Sugarloaf Diorite

Sugarloaf diorite has the least surface exposure of the Iron Mask batholith phases and forms the western margin of the batholith. The Sugarloaf phase hosts the past-producing Pothook and Ajax deposits. Sample 20TL-BC-IMR4 was collected from a roadcut on the southeastern margin of the batholith, east of the Ajax open pits. The outcrop is dark grey and mostly fresh.

The fresh rock is a dark greenish grey, porphyritic, plagioclase- and hornblende-phyric diorite (Figure 3c). It is composed of creamy white, 1–2 mm, round anhedral and tabular euhedral plagioclase phenocrysts (25%); 1–3 mm, dark green, anhedral hornblende phenocrysts (10%); translucent anhedral quartz eyes (1%); small, shiny, black euhedral magnetite (1%); and a groundmass of dark grey-

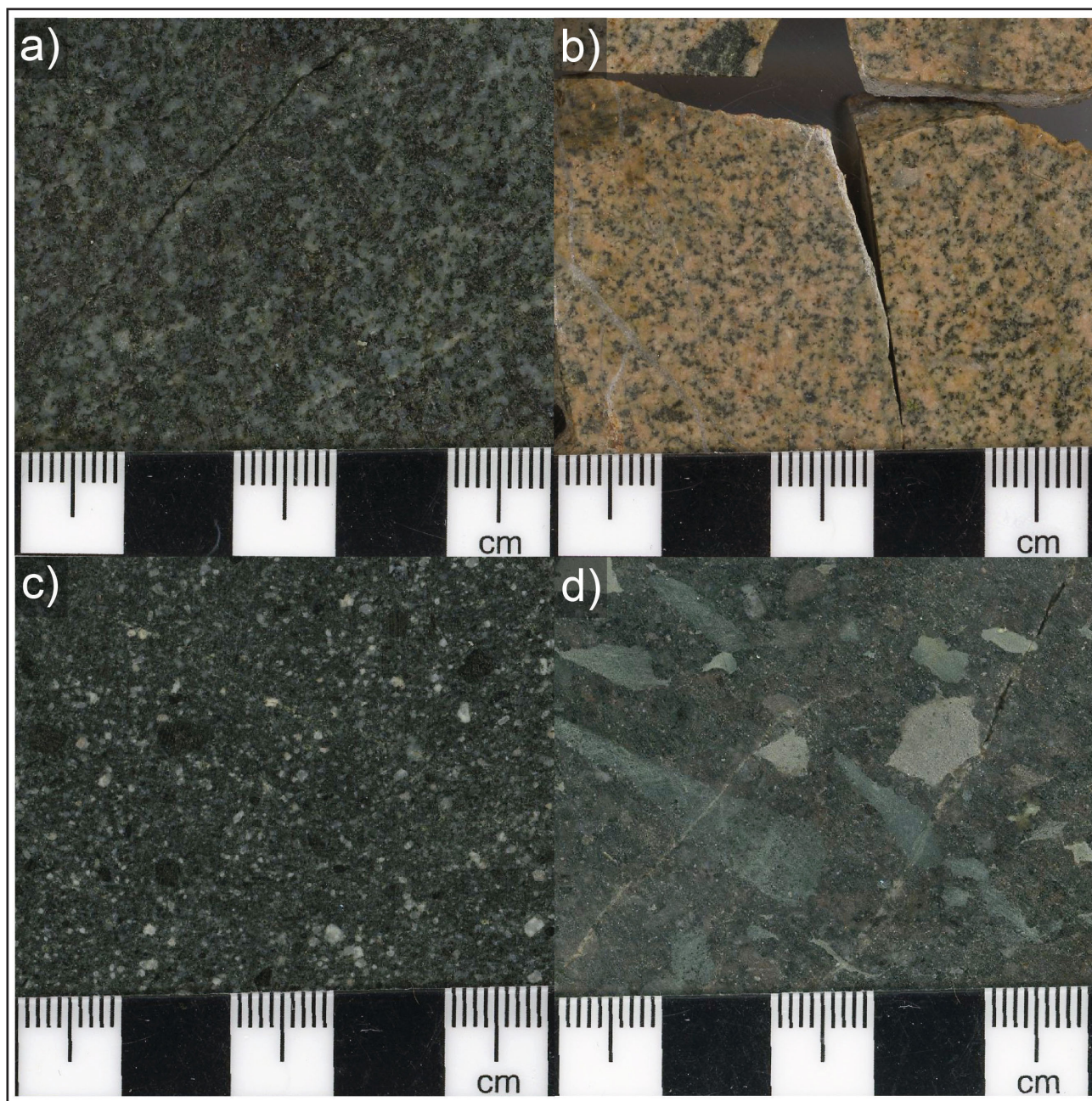


Figure 3. Rocks of the Iron Mask batholith in the alkaline Central magmatic axis: **a)** diorite of the Pothook phase, **b)** equigranular monzonite of the Cherry Creek phase, **c)** porphyritic diorite of the Sugarloaf phase, and **d)** xenolith-rich diorite of the Hybrid phase.

green, fine-grained mafic minerals (42%). It locally contains 1–2 cm xenoliths of fine-grained, strongly chloritized, Nicola group volcanic rocks (5%). Mafic minerals are strongly chloritized and there are multiple clusters of the mafic groundmass that are almost completely replaced by epidote. The rock has a magnetic susceptibility of 39.81×10^{-3} SI.

Hybrid Phase

The hybrid phase is a xenolith-rich, heterogenous unit that forms about half of the surface exposure of the Iron Mask

batholith. Hybrid rocks mark the contacts between the individual phases of the batholith and can locally have a matrix consisting of all the phases in the batholith (Logan and Mihalynuk, 2005). Sample 20TL-BC-IMR5 was collected as a rounded clast in glacial till near the centre of the batholith.

The fresh rock is a pinkish green, xenolith-rich, fine-grained, equigranular diorite (Figure 3d). It is composed of 2–10 mm angular clasts of volcanic and sedimentary Nicola Group xenoliths (37%), dark green poikilitic biotite

(30%), creamy white subhedral plagioclase (22%), creamy orange anhedral alkali feldspar (4%), translucent anhedral quartz (2%) and trace magnetite. The rock is strongly altered to albite. It has a magnetic susceptibility of 1.19×10^{-3} SI.

Till Samples

Most of the Iron Mask Batholith is covered by a glacial-till veneer that was transported to the southeast (Fulton, 1963). Three till samples were taken progressively farther south and down ice from each other.

Sample 20TL-BC-IMT1 was collected at the northeast edge of the batholith, 3 km east of the Afton mine. It is composed of clay (47%), silt (30%) sand (10%), subrounded, pebble-size (2–40 mm) clasts of Nicola Group volcanic rocks (10%) and subrounded to angular, pebble- to cobble-size (20–80 mm) clasts of monzonite and lesser diorite (3%).

Sample 20TL-BC-IMT2 was collected near the centre of the batholith, southeast of Sugarloaf hill (unofficial place name; UTM Zone 10U, 678753E, 5612737N, NAD 83). The sample is composed of clay (45%), silt (33%), sand (10%) and subrounded to angular, pebble- to cobble-size (10–80 mm) clasts of mostly diorite with lesser amounts of xenolith-rich hybrid phase and monzonite (8%), and subrounded, pebble-size (2–30 mm) clasts of Nicola Group volcanic rocks (4%).

Sample 20TL-BC-IMT3 was collected near the south-central portion of the batholith, 1 km southeast of the Ajax deposits. It is composed of clay (42%), silt (35%), sand (10%) and subrounded to angular, pebble- to cobble-size (10–50 mm) clasts of mostly diorite with lesser amounts of monzonite and xenolith-rich hybrid phase (10%), and subrounded, pebble-size (2–20 mm) clasts of Nicola Group volcanic rocks (3%).

Eastern Magmatic Axis (Calcalkaline, Granodiorite Suite)

Pennask Batholith

Brenda Stock

Sample 20TL-BC-PR1 was collected from the southwest side of the Trepanier Creek ravine 6 km east of the past-producing Brenda Cu-Mo mine. The outcrop was weathered a brownish grey colour and strongly fractured.

The fresh rock is light brownish grey, hypidiomorphic, equigranular, coarse-grained, hornblende-biotite granodiorite (Figure 4a). It is composed of creamy white subhedral plagioclase (40%), translucent subhedral quartz (28%), creamy orange subhedral alkali feldspar (18%), greenish black subhedral biotite (8%), black euhedral acicular needles of hornblende (6%) and trace magnetite. Plagioclase is weakly sericitized, biotite is weakly

chloritized and there are several quartz veinlets with sericite alteration selvages. The rock has a magnetic susceptibility of 18.03×10^{-3} SI.

Till Sample

Sample 20TL-BC-PT1 was collected from a bank along a roadcut 4 km southeast of the Brenda mine and downslope of the Brenda tailings dam. This till is likely sourced from the Pennask batholith, located up ice to the north. The sample is graded and composed of sand (50%), pebbles (20%), silt (15%) and clay (15%).

Stream-Sediment Sample

Sample 20TL-BC-PF1 was collected from Trepanier Creek, which drains the northern half of the Pennask batholith, 8 km east of the Brenda mine. The sample is composed of fine-grained sand (60%), silt (30%) and small pebbles (10%).

Bromley Batholith

The fresh rock is a light creamy pink, coarse-grained, hypidiomorphic, inequigranular hornblende granodiorite (Figure 4b). It is composed of creamy white subhedral plagioclase (44%), translucent subhedral quartz (30%), creamy orange subhedral alkali feldspar (10%), greenish black, euhedral, acicular needles of hornblende (15%) and small, shiny, black euhedral grains of magnetite (1%). Feldspars are weakly sericitized, hornblende is weakly chloritized and locally altered to epidote. There are several quartz veinlets with sericite alteration selvages bordering the vein margins. The rock has a magnetic susceptibility of 21.0×10^{-3} SI.

Cahill Creek Pluton

The fresh rock is a light creamy pink, coarse-grained, inequigranular, xenolith-bearing, hornblende-biotite granite (Figure 4c). It is composed of creamy white subhedral plagioclase (25%), pinkish orange subhedral alkali feldspar (19%), translucent subhedral quartz (20%), black subhedral biotite (3%), black acicular hornblende (2%) and irregular 1–40 mm xenoliths of a fine- to medium-grained clinopyroxene-hornblende quartz diorite (30%), possibly from the Hedley intrusion. Feldspars are moderately sericitized and there are several chlorite veinlets with sericite alteration selvages bordering the vein margins. The rock has a magnetic susceptibility of 14.36×10^{-3} SI.

Hedley Intrusion

The fresh rock is a dark green, medium-grained, equigranular, pyroxene-hornblende quartz diorite (Figure 4d). It is composed of creamy white subhedral plagioclase (25%), black subhedral hornblende (30%), green euhedral clinopyroxene (25%), translucent subhedral quartz eyes (8%), creamy orange subhedral alkali feldspar (2%) and trace magnetite. Plagioclase is moderately sericitized and hornblende is weakly chloritized,

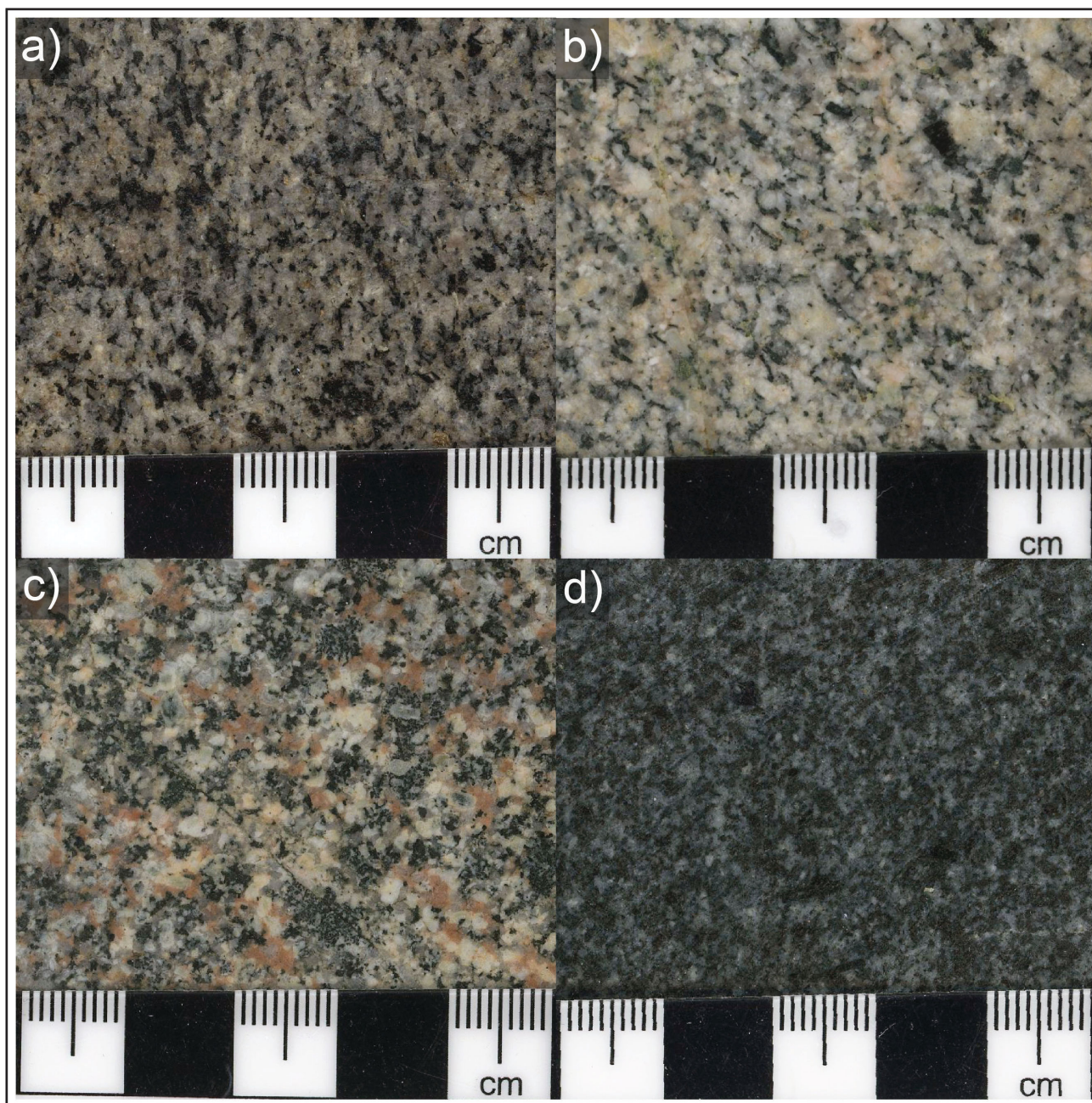


Figure 4. Rocks of the calcalkaline Eastern magmatic axis: **a)** equigranular granodiorite of the Brenda stock, Pennask batholith; **b)** inequigranular granodiorite of the Bromley pluton, **c)** inequigranular granite of the Cahill Creek pluton, and **d)** equigranular diorite of the Hedley intrusion.

and there are a few calcite-chlorite veinlets. The rock has a magnetic susceptibility of 0.84×10^{-3} SI.

Future Sample Processing and Analysis

Samples will be crushed, sieved, washed and hand-panned prior to heavy-liquid separation using methylene iodide solution to separate them into heavy and light fractions. Approximately 30–50 zircons will be picked from each rock sample and 100–200 zircons from each stream-sediment and till sample, and mounted in an epoxy puck. Zircons will

be imaged in reflected light and cathodoluminescence, and the morphology of the crystals will be classified to identify zircon populations with characteristic habit and growth bands. Appropriate inclusion-free spots will be chosen and analyzed at The University of British Columbia Pacific Centre for Isotopic and Geochemical Research using laser-ablation inductively coupled plasma–mass spectrometry (LA-ICP-MS) to determine the trace-element composition as well as the U-Pb dates. Zircon cores and rims will both be analyzed in each sample when possible. Alkali feldspars will be picked from the light fraction and mounted on a

puck to be analyzed for composition and Pb isotopes via LA-ICP-MS. A fresh portion of the rock samples will be analyzed for major oxides, trace elements and iron speciation.

Summary

There is a very strong geological and geochronological framework that documents the changes in the Quesnellia arc throughout time, resulting in varying magma chemistries, emplacement depths, and styles of plutons and associated porphyry mineralization (Mortensen et al., 1995; McMillan et al., 1996; Logan et al., 2011; Logan and Mihalynuk, 2014; Schiarizza, 2014). This provides a foundation upon which investigations of variability in magmatic porphyry fertility throughout arc evolution can be undertaken, in this case by evaluating the chemistry of zircons.

Glacial-till and stream-sediment samples have been taken to test the effectiveness of using detrital zircons as an exploration tool, and as a means to increase the zircon representation of the arc and to increase the potential for obtaining zircons from silica-undersaturated to weakly silica-saturated intrusions that typically have low zircon yields.

The ability to identify fertile arc magmas and understand variability within and between different arc settings will enable explorers to better recognize magmas with the potential to form an economic porphyry Cu deposit and differentiate them from barren intrusions. This research will be applied to develop an exploration toolkit for porphyry Cu deposits that uses detrital and primary zircons to characterize the magmatic fertility of a district or belt to improve explorers' ability to discover economic porphyry mineralization beneath cover.

Acknowledgments

This project is part of the Mineral Deposit Research Unit's Porphyry Indicator Minerals (PIMS) project. Geoscience BC is thanked for its financial contribution in support of this project in the form of a 2020 Geoscience BC Scholarship. Additional funding was provided by the Society of Economic Geologists Canada. The authors thank R.G. Lee for his comments, insights, and suggestions for improvement.

References

Ager, C.A. (1974): The three-dimensional structure of batholiths as deduced from gravity data; Ph.D. thesis, The University of British Columbia, 143 p., URL <<https://doi.org/10.14288/1.0052998>>.

Ash, C.H. and Riveros, C.P. (2001): Geology of the Gibraltar copper-molybdenite deposit, east-central British Columbia (93B/9); *in* Geological Fieldwork 2000, BC Ministry of Energy, Mines and Low Carbon Innovation, BC Geological Survey, Paper 2001-1, p. 119–133, URL <[http://](http://cmscontent.nrs.gov.bc.ca/geoscience/PublicationCatalogue/Paper/BCGS_P2001-01-09_Ash.pdf)

cmscontent.nrs.gov.bc.ca/geoscience/PublicationCatalogue/Paper/BCGS_P2001-01-09_Ash.pdf> [October 2020].

- Ash, C.H., Reynolds, P.H., Creaser, R.A. and Mihalynuk, M.G. (2007): $^{40}\text{Ar}/^{39}\text{Ar}$ and Re-Os isotopic ages for hydrothermal alteration and related mineralization at the Highland Valley Cu-Mo deposit (NTS 092I), southwestern British Columbia; *in* Geological Fieldwork 2006, BC Ministry of Energy, Mines and Low Carbon Innovation, BC Geological Survey, Paper 2007-1, p. 19–24, URL <http://cmscontent.nrs.gov.bc.ca/geoscience/PublicationCatalogue/Paper/BCGS_P2007-01-02_Ash.pdf> [October 2020].
- Ballard, J.R., Palin, M.J. and Campbell, I.H. (2002): Relative oxidation states of magmas inferred from Ce(IV)/Ce(III) in zircon: application to porphyry copper deposits of northern Chile; *Contributions to Mineralogy and Petrology*, v. 144, p. 347–364, URL <<https://doi.org/10.1007/s00410-002-0402-5>>.
- BC Geological Survey (2020): MINFILE BC mineral deposits database; BC Ministry of Energy, Mines and Low Carbon Innovation, BC Geological Survey, URL <<http://minfile.ca/>> [October 2020].
- Belousova, E.A., Griffin, W.L. and O'Reilly, S.Y. 2006. Zircon crystal morphology, trace element signatures and Hf isotope composition as a tool for petrogenetic modelling: examples from eastern Australian granitoids; *Journal of Petrology*, v. 47, p. 329–353, URL <<https://doi.org/10.1093/petrology/egi077>>.
- Bouzari, F., Hart, C.J.R. and Bissig, T. (2020): Assessing British Columbia porphyry fertility in British Columbia batholiths using zircons; Geoscience BC Report 2020-07, MD RU Publication 450, 24 p.
- Bouzari, F., Hart, C.J.R., Bissig, T. and Barker, S. (2016): Hydrothermal alteration revealed by apatite luminescence and chemistry: a potential indicator mineral for exploring covered porphyry copper deposits; *Economic Geology*, v. 111, p. 1397–1410, URL <<https://doi.org/10.2113/econgeo.111.6.1397>>.
- Burnham, C.W. and Ohmoto, H. (1980): Late stage processes of felsic magmatism; *in* Granitic Magmatism and Related Mineralization, S. Ishihara and S. Takenouchi (ed.), Society of Mining Geologists of Japan, Special Issue 8, p. 1–11.
- Byrne, K., Stock, E., Ryan, J., Johnson, C., Nisenson, J., Alva Jimenez, T., Lapointe, M., Stewart, H., Grubisa, G. and Sykora, S. (2013): Porphyry Cu-(Mo) deposits in the Highland Valley district, south-central British Columbia; Society of Economic Geologists, Field Trip Guidebook Series, v. 43, p. 99–116.
- Bysouth, G.D., Campbell, K.V., Barker, G.E. and Gagnier, G.K. (1995): Tonalite trondhjemite fractionation of peraluminous magma and the formation of syntectonic porphyry copper mineralization, Gibraltar mine, central British Columbia; *in* Porphyry Deposits of the Northwestern Cordillera of North America, T.G. Schroeter (ed.), Canadian Institute of Mining, Metallurgy and Petroleum, Special Volume 46, p. 201–213.
- Celis, A. (2015): Titanite as an indicator mineral for alkalic porphyry Cu-Au deposits in south-central British Columbia; M.Sc. thesis, The University of British Columbia, 247 p., URL <<https://doi.org/10.14288/1.0166663>>.
- Colpron, M. and Nelson, J.L. (2020): A digital atlas of terranes for the northern Cordillera; Yukon Geological Survey, URL <<http://data.geology.gov.yk.ca/Compilation/2>> [October 2020].

- Colpron, M. and Price, R.A. (1995): Tectonic significance of the Kootenay terrane, southeastern Canadian Cordillera: an alternative model; *Geology*, v. 23, p. 25–28, URL <[https://doi.org/10.1130/0091-7613\(1995\)023<0025:TSOT-KT>2.3.CO;2](https://doi.org/10.1130/0091-7613(1995)023<0025:TSOT-KT>2.3.CO;2)>.
- Consolidated Woodjam Copper Corp. (2013): Woodjam projects; Consolidated Woodjam Copper Corp., URL <<https://www.woodjamcopper.com/projects/>> [October 2020].
- Copper Mountain Mining Corp. (2020): Mineral reserve and mineral resource for the Copper Mountain operation; Copper Mountain Mining Corp., URL <<https://www.cumtn.com/operations/copper-mountain-mine/overview/>> [October 2020].
- Cui, Y., Miller, D., Schiarizza, P. and Diakow, L.J. (2017): British Columbia digital geology; BC Ministry of Energy, Mines and Low Carbon Innovation, BC Geological Survey, Open File 2017-8, 9 p., URL <http://cmscontent.nrs.gov.bc.ca/geoscience/PublicationCatalogue/OpenFile/BCGS_OF-2017-08.pdf> [October 2020].
- D'Angelo, M. (2016): Geochemistry, petrography and mineral chemistry of the Guichon Creek and Nicola batholiths, south-central British Columbia; M.Sc. thesis, Lakehead University, 435 p.
- D'Angelo, M., Miguel, A., Hollings, P., Byrne, K., Piercey, S. and Creaser, R. (2017): Petrogenesis and magmatic evolution of the Guichon Creek batholith: Highland Valley porphyry Cu±(Mo) district, south-central British Columbia; *Economic Geology*, v. 112, p. 1857–1888, URL <<https://doi.org/10.5382/econgeo.2017.4532>>.
- del Real, I., Bouzari, F., Rainbow, A., Bissig, T., Blackwell, J., Sherlock, R., Thompson, J.F.H. and Hart, C.J.R. (2017): Spatially and temporally associated porphyry deposits with distinct Cu/Au/Mo ratios, Woodjam district, central British Columbia; *Economic Geology*, v. 112, p. 1673–1717, URL <<https://doi.org/10.5382/econgeo.2017.4526>>.
- Dilles, J.H. and Einaudi, M.T. (1992): Wall-rock alteration and hydrothermal flow paths about the Ann-Mason porphyry copper deposit, Nevada – a 6-km vertical reconstruction; *Economic Geology*, v. 87, p. 1963–2001, URL <<https://doi.org/10.2113/gsecongeo.87.8.1963>>.
- Dilles, J.H., Kent, A.J.R., Wooden, J.L., Tosdal, R.M., Koleszar, A., Lee, R.G. and Farmer, L.P. (2015): Zircon compositional evidence for sulfur-degassing from ore-forming arc magmas; *Economic Geology*, v. 110, p. 241–251, URL <<https://doi.org/10.2113/econgeo.110.1.241>>.
- Fulton, R.J. (1963): Surficial geology, Kamloops Lake, British Columbia; Geological Survey of Canada, Map 9-1963, 1 sheet, 1:126 720 scale., URL <<https://doi.org/10.4095/108672>>.
- Ghaffari, H., Stubens, T.C., de Ruijter, A., Ulansky, R., Borntraeger, B. and Newcomen, H.W. (2009): Ajax copper/gold project, Kamloops, British Columbia – preliminary assessment technical report, July 31, 2009; Abacus Mining and Exploration Corp., 172 p., URL <https://www.amemining.com/site/assets/files/5750/2009-08-05_ajaxpatechnicalreport.pdf> [November 2020].
- Harding, B. (2012): The characterization of molybdenum mineralization at the Gibraltar mines Cu-Mo porphyry, central British Columbia; B.Sc. thesis, Queen's University, 52 p.
- Holbek, P. and Joyes, R. (2013). Copper Mountain: an alkalic porphyry copper-gold-silver deposit in the southern Quesnel terrane, British Columbia; *in* Porphyry Systems of Central and Southern BC: Tour of Central BC Porphyry Deposits from Prince George to Princeton, J.M. Logan and T.G. Schroeter (ed.), Society of Economic Geologists, Field Trip Guidebook Series, v. 44, p. 129–143.
- International Copper Study Group (2019): The World Copper Factbook 2019; International Copper Study Group, URL <<https://www.icsg.org/index.php/component/jdownloads/finish/170/3046>> [October 2020].
- Kobylinski, C., Hattori, K., Smith, S. and Plouffe, A. (2020): Protracted magmatism and mineralized hydrothermal activity at the Gibraltar porphyry copper-molybdenum deposit, British Columbia; *Economic Geology*, v. 115, no. 5, p. 1119–1136, URL <<https://doi.org/doi:10.5382/econgeo.4724>>.
- Lang, J.R., and Stanley, C.R. (1995): Contrasting styles of alkalic porphyry copper-gold deposits in the northern Iron Mask batholith, Kamloops, British Columbia; Canadian Institute of Mining, Metallurgy and Petroleum, Special Volume 46, p. 581–592.
- Lang, J.R., Lueck, B., Mortensen, J.K., Russell, J.K., Stanley, C.R. and Thompson, J.F.H. (1995): Triassic–Jurassic silica-undersaturated and silica-saturated alkalic intrusions in the Cordillera of British Columbia: implications for arc magmatism; *Geology*, v. 23, p. 451–454, URL <[https://doi.org/10.1130/0091-7613\(1995\)023<0451:TJS-UAS>2.3.CO;2](https://doi.org/10.1130/0091-7613(1995)023<0451:TJS-UAS>2.3.CO;2)>.
- Lee, R.G. (2008): Genesis of the El Salvador porphyry copper deposit, Chile and distribution of epithermal alteration at Lassen Peak, California; Ph.D. thesis, Oregon State University, 344 p.
- Lee, R.G., Bryne, K., D'Angelo, M.D., Hart, C.J.R., Hollings, P., Gleeson, S.A. and Alfaro, M. (2020): Using zircon trace element composition to assess porphyry copper potential of the Guichon Creek batholith and Highland Valley Copper deposit, south-central British Columbia; *Mineralium Deposita*, URL <<https://doi.org/10.1007/s00126-020-00961-1>>.
- Lee, R.G., Dilles, J.H., Tosdal, R.M., Wooden, J.L. and Mazdab, F.K. (2017): Magmatic evolution of granodiorite intrusions at the El Salvador porphyry copper deposit, Chile, based on trace element composition and U/Pb age of zircons; *Economic Geology*, v. 112, p. 245–273, URL <<https://doi.org/10.2113/econgeo.112.2.245>>.
- Lee, R.G., Plouffe, A., Ferbey, T., Hart, C.J.R., Hollings, P. and Gleeson, S.A. (in press): Recognizing porphyry copper potential from till zircon composition: a case study from the Highland Valley porphyry district, south-central British Columbia; *Economic Geology Scientific Communications*, accepted for publication.
- Little, H.W. (1960): Nelson map-area, west half, British Columbia (82F W1/2); Geological Survey of Canada, Memoir 308, 205 p., URL <<https://doi.org/10.4095/100535>>.
- Logan, J.M. and Mihalynuk, M.G. (2005): Porphyry Cu-Au deposits of the Iron Mask batholith, southeastern British Columbia; *in* Geological Fieldwork 2004, BC Ministry of Energy, Mines and Low Carbon Innovation, BC Geological Survey, Paper 2005-1, p. 249–270, URL <http://cmscontent.nrs.gov.bc.ca/geoscience/PublicationCatalogue/Paper/BCGS_P2005-RR07_Logan.pdf> [October 2020].
- Logan, J.M. and Mihalynuk, M.G. (2014): Tectonic controls on Early Mesozoic paired alkaline porphyry deposit belts (Cu-Au ± Ag-Pt-Pd-Mo) within the Canadian Cordillera; *Economic Geology*, v. 109, p. 827–858, URL <<https://doi.org/10.2113/econgeo.109.4.827>>.

- Logan, J.M., Mihalynuk, M.G., Friedman, R.M. and Creaser, R.A. (2011): Age constraints of mineralization at the Brenda and Woodjam Cu-Mo±Au porphyry deposits – an Early Jurassic calcalkaline event, south-central British Columbia; *in* Geological Fieldwork 2010, BC Ministry of Energy, Mines and Low Carbon Innovation, BC Geological Survey, Paper 2011-01, p. 129–144, URL <http://cmscontent.nrs.gov.bc.ca/geoscience/PublicationCatalogue/Paper/BCGS_P2011-01-09_Logan.pdf> [October 2020].
- Logan, J.M., Mihalynuk, M.G., Ullrich, T. and Friedman, R.M. (2007): U-Pb ages of intrusive rocks and ⁴⁰Ar/³⁹Ar plateau ages of copper-gold-silver mineralization associated with alkaline intrusive centres at Mount Polley and the Iron Mask batholith, southern and central British Columbia; *in* Geological Fieldwork 2006, BC Ministry of Energy, Mines and Low Carbon Innovation, BC Geological Survey, Paper 2007-1, p. 93–116, URL <http://cmscontent.nrs.gov.bc.ca/geoscience/PublicationCatalogue/Paper/BCGS_P2007-01-10_Logan.pdf> [October 2020].
- Lu, Y., Loucks, R.R., Fiorentini, M., McCuaig, T.C., Evans, N.J., Yang, Z., Hou, Z., Kirkland, C.L., Parra-avila, L.A. and Kobussen, A. (2016): Zircon compositions as a pathfinder for porphyry Cu ± Mo ± Au deposits; *Economic Geology Special Publications*, v. 19, p. 329–347.
- McMillan, W.J. (1976): Geology and genesis of the Highland Valley ore deposits and the Guichon Creek batholith; *in* Porphyry Deposits of the Canadian Cordillera, A. Sutherland Brown (ed.), Canadian Institute of Mining and Metallurgy, Special Volume 15, p. 85–104.
- McMillan, W.J. (1981): Nicola project – Merritt area; BC Ministry of Energy, Mines and Low Carbon Innovation, BC Geological Survey, Preliminary Map 47 (2 sheets), scale 1:25 000, URL <http://cmscontent.nrs.gov.bc.ca/geoscience/PublicationCatalogue/PreliminaryMap/BCGS_PM47.pdf> [October 2020].
- McMillan, W.J. (1985): Geology and ore deposits of the Highland Valley camp; Field Guide and Reference Manual Series, A.J. Sinclair (ser. ed.), Geological Association of Canada, Mineral Deposits Division, no. 1, 121 p.
- McMillan, W.J., Thompson, J.F.H., Hart, C.J.R. and Johnston, S.T. (1996): Porphyry deposits of the Canadian Cordillera; *Geoscience Canada*, v. 23, p. 125–134.
- Monger, J.W.H. (1985): Structural evolution of the southwestern Intermontane belt, Ashcroft and Hope map areas, British Columbia; *in* Current Research, Part A, Geological Survey of Canada, Paper 85-1A, p. 349–3523.
- Mortensen, J.K., Ghosh, D.K. and Ferri, F. (1995): U-Pb geochronology of intrusive rocks associated with copper-gold porphyry deposits in the Canadian Cordillera; *in* Porphyry Deposits of the Northwestern Cordillera of North America, T.G. Schroeter (ed.), Canadian Institute of Mining, Metallurgy and Petroleum, Special Volume 46, p. 142–158.
- Mortimer, N. (1987): The Nicola Group: Late Triassic and Early Jurassic subduction-related volcanism in British Columbia; *Canadian Journal of Earth Sciences*, v. 24, p. 2521–2536, URL <<https://doi.org/10.1139/e87-236>>.
- New Gold Inc. (2019): New Gold mineral reserves and resources summary on December 31, 2019; New Gold Inc., URL <<https://www.newgold.com/investors/financial-information/reserves-and-resources/default.aspx>> [October 2020].
- Nixon, G.T., Archibald, D.A. and Heaman, L.M. (1993): ⁴⁰Ar-³⁹Ar and U-Pb geochronometry of the Polaris Alaskan type complex, British Columbia: precise timing of Quesnellia–North America interaction, Geological Association of Canada–Mineralogical Association of Canada, Joint Annual Meeting, Waterloo, Ontario, Program with Abstracts, p. 76.
- Northcote, K.E. (1969): Geology and geochronology of the Guichon Creek Batholith; BC Ministry of Energy, Mines and Low Carbon Innovation, BC Geological Survey, Bulletin 56, 77 p., URL <http://cmscontent.nrs.gov.bc.ca/geoscience/PublicationCatalogue/Bulletin/BCGS_B-056.pdf> [October 2020].
- Northcote, K.E. (1978): Iron Mask batholith (92 119, 10); *in* Geological Fieldwork 1977, BC Ministry of Energy, Mines and Low Carbon Innovation, BC Geological Survey, Paper 1978-01, p. 37–38.
- Natural Resources Canada. (2018): Canadian mine production of copper, by province and territory, 2018, URL <<https://www.nrcan.gc.ca/our-natural-resources/minerals-mining/copper-facts/20506#L2>> [October 2020].
- Panteleyev, A. (1978): Granite Mountain project (93B/8); *in* Geological Fieldwork 1977, BC Ministry of Energy, Mines and Low Carbon Innovation, BC Geological Survey, Paper 1977-1, p. 39–42.
- Parrish, R.R. and Monger, J.W.H. (1992): New U-Pb dates from southwestern British Columbia; *in* Radiogenic Age and Isotopic Studies, Report 5, Geological Survey of Canada, p. 87–108.
- Pizarro, H., Campos, E., Bouzari, F., Rousse, S., Bissig, T., Gregoire, M. and Riquelme, R. (2020): Porphyry indicator zircons (PIZs): application to exploration of porphyry copper deposits; *Ore Geology Reviews*, v. 126, URL <<https://doi.org/10.1016/j.oregeorev.2020.103771>>.
- Preto, V.A. (1972): Geology of Copper Mountain, British Columbia; BC Ministry of Energy, Mines and Low Carbon Innovation, BC Geological Survey, Bulletin 59, 87 p., URL <http://cmscontent.nrs.gov.bc.ca/geoscience/PublicationCatalogue/Bulletin/BCGS_B059.pdf> [October 2020].
- Preto, V.A. (1979): Geology of the Nicola Group between Merritt and Princeton; BC Ministry of Energy, Mines and Low Carbon Innovation, BC Geological Survey, Bulletin 69, 90 p., URL <http://cmscontent.nrs.gov.bc.ca/geoscience/PublicationCatalogue/Bulletin/BCGS_B069.pdf> [October 2020].
- PricewaterhouseCoopers Inc. (2019): ESG: Resilience and opportunity in uncertain times – the mining industry in British Columbia 2019; PricewaterhouseCoopers Canada, URL <<https://www.pwc.com/ca/en/mining/publications/p688279-bc-mines-report-2019-report-en.pdf#page=8>> [November 2020].
- Read, P.B. and Okulitch, A.V. (1977): The Triassic unconformity of south-central British Columbia; *Canadian Journal of Earth Sciences*, v. 14, p. 606–638, URL <<https://doi.org/10.1139/e77-063>>.
- Rezeau, H., Moritz, R., Wotzlaw, J.-F., Hovakimyan, S. and Tayan, R. (2019): Zircon petrochronology in the ore-bearing Meghri-Ordubad pluton, Lesser Caucasus: fingerprinting igneous processes with implications for the exploration of porphyry Cu-Mo deposits; *Economic Geology*, v. 114, p. 1365–1388, URL <<https://doi.org/10.5382/econgeo.4671>>.
- Schiarizza, P. (2014): Geological setting of the Granite Mountain batholith, host to the Gibraltar porphyry Cu-Mo deposit, south-central British Columbia; *in* Geological Fieldwork 2013, BC Ministry of Energy, Mines and Low Carbon Innovation, BC Geological Survey, Paper 2014-1, p. 95–110,

- URL <http://cmscontent.nrs.gov.bc.ca/geoscience/PublicationCatalogue/Paper/BCGS_P2014-01-06_Schiarizza.pdf> [October 2020].
- Schiarizza, P. (2015): Geological setting of the Granite Mountain batholith, south-central British Columbia; *in* Geological Fieldwork 2014, BC Ministry of Energy, Mines and Low Carbon Innovation, BC Geological Survey, Paper 2015-1, p. 19-39, URL <http://cmscontent.nrs.gov.bc.ca/geoscience/PublicationCatalogue/Paper/BCGS_P2015-01-02_Schiarizza.pdf> [October 2020].
- Schiarizza, P. (2016): Toward a regional stratigraphic framework for the Nicola Group: preliminary results from the Bridge Lake–Quesnel River area; *in* Geological Fieldwork 2015, BC Ministry of Energy, Mines and Low Carbon Innovation, BC Geological Survey, Paper 2016-1, p. 13–30, URL <http://cmscontent.nrs.gov.bc.ca/geoscience/PublicationCatalogue/Paper/BCGS_P2016-01-02_Schiarizza.pdf> [October 2020].
- Schiarizza, P. (2019): Geology of the Nicola Group in the Bridge Lake–Quesnel River area, south-central British Columbia; *in* Geological Fieldwork 2018, BC Ministry of Energy, Mines and Low Carbon Innovation, BC Geological Survey, Paper 2019-01, p. 15–30, URL <http://cmscontent.nrs.gov.bc.ca/geoscience/PublicationCatalogue/Paper/BCGS_P2019-01-02_Schiarizza.pdf> [October 2020].
- Schiarizza, P., Bell, K. and Bayliss, S. (2009): Geology and mineral occurrences of the Murphy Lake area, south-central British Columbia (NTS 93A/03); *in* Geological Fieldwork 2013, BC Ministry of Energy, Mines and Low Carbon Innovation, BC Geological Survey, Paper 2014-1, p. 95–110, URL <http://cmscontent.nrs.gov.bc.ca/geoscience/PublicationCatalogue/Paper/BCGS_P2009-01-15_Schiarizza.pdf> [October 2020].
- Schiarizza, P., Israel, S., Heffernan, S., Boulton, A., Bligh, J., Bell, K., Bayliss, S., Macauley, J., Bluemel, B., Zuber, J., Friedman, R.M., Orchard, M.J. and Poulton, T.P. (2013): Bedrock geology between Thuya and Woodjam creeks, south-central British Columbia, NTS 92P/7, 8, 9, 10, 14, 15, 16; 93A/2, 3, 6; BC Ministry of Energy, Mines and Low Carbon Innovation, BC Geological Survey, Open File 2013-05; 4 sheets, scale 1:100 000, URL <http://cmscontent.nrs.gov.bc.ca/geoscience/PublicationCatalogue/OpenFile/BCGS_OF2013-05.pdf> [October 2020].
- Shen, P., Hattori, K., Pan, H., Jackson, S. and Seitmuratova, E. (2015): Oxidation condition and metal fertility of granitic magmas: zircon trace-element data from porphyry Cu deposits in the central Asian orogenic belt; *Economic Geology*, v. 110, p. 1861–1878, URL <<https://doi.org/10.2113/econgeo.110.7.1861>>.
- Smith, R.B. (1979): Geology of the Harper Ranch Group (Carboniferous–Permian) and Nicola Group (Upper Triassic) north-east of Kamloops, British Columbia; M.Sc. thesis, The University of British Columbia, 211 p., URL <<https://doi.org/10.14288/1.0052516>>.
- Snyder, L.D. and Russell, J.K. (1995): Petrogenetic relationships and assimilation processes in the alkalic Iron Mask Batholith, south-central British Columbia; *in* Porphyry Deposits of the Northwestern Cordillera of North America, Schroeter, T.G. (ed.), Canadian Institute of Mining, Metallurgy and Petroleum, Special Volume 46, p. 593–608.
- Soregaroli, A.E. and Whitford, D.F. (1976): Brenda; *in* Porphyry Deposits of the Canadian Cordillera, A. Sutherland Brown (ed.), Canadian Institute of Mining and Metallurgy, Special Volume 15, p. 186–194.
- Struik, L.C. (1988): Regional imbrication within Quesnel Terrane, central British Columbia, as suggested by conodont ages; *Canadian Journal of Earth Sciences*, v. 25, p. 1608–1617, URL <<https://doi.org/10.1139/e88-153>>.
- Sutherland Brown, A., editor (1976): Porphyry deposits of the Canadian Cordillera; Canadian Institute of Mining, Metallurgy and Petroleum, Special Volume 15, 510 p.
- Teck Resources Limited (2019): Annual information form; Teck Resources Limited, public filing, URL <<https://www.teck.com/investors/reserves-&-resources/reserves-and-resources>> [October 2020].
- Thomas, M.D. (2019): Gravity and magnetic models of the Iron Mask Batholith, south-central Canadian Cordillera, British Columbia; Geological Survey of Canada, Current Research 2019-1, 24 p., URL <<https://doi.org/10.4095/314517>>.
- Travers, W.B. (1978): Overturned Nicola and Ashcroft strata and their relations to the Cache Creek Group, southwestern Intermontane belt, British Columbia; *Canadian Journal of Earth Sciences*, v. 15, p. 99–116, URL <<https://doi.org/10.1139/e78-009>>.
- Wainwright, A.J., Tosdal, R.M., Wooden, J.L., Mazdab, F.K. and Friedman, R.M. (2011): U-Pb (zircon) and geochemical constraints on the age, origin, and evolution of Paleozoic arc magmas in the Oyu Tolgoi porphyry Cu-Au district, southern Mongolia; *Gondwana Research*, v. 19, p. 764–787, URL <<https://doi.org/10.1016/j.gr.2010.11.012>>.
- Weymark, R. (2019): Technical report on the mineral reserve update at the Gibraltar mine, British Columbia, Canada, 228 p., URL <http://www.sedar.com/issuers/issuers_en.htm> [October 2020].
- Weeks, R.M., Bradburn, R.G., Flintoff, B.C., Harris, G.R. and Malcolm, G. (1995): The Brenda mine: the life of a low-cost porphyry copper-molybdenum producer (1970–1990), southern British Columbia, *in* Porphyry Deposits of the Northwestern Cordillera of North America, T.G. Schroeter (ed.), Canadian Institute of Mining and Metallurgy, Special Volume 46, p. 192–200.
- Williamson, B.J., Herrington, R.J. and Morris, A. (2016): Porphyry copper enrichment linked to excess aluminium in plagioclase; *Nature Geosciences*, v. 9, p. 237–242, URL <<https://doi.org/10.1038/ngeo2651>>.
- Whiteaker, R.J., Mortensen, J.K. and Friedman, R.M. (1998): U-Pb geochronology, Pb isotopic signatures and geochemistry of an Early Jurassic alkalic porphyry system near Lac La Hache; *in* Geological Fieldwork 1997, BC Ministry of Energy, Mines and Low Carbon Innovation, BC Geological Survey, Paper 1998-01, p. 33-1–33-14.

